ELSEVIER

Engineering Geology 41 (1996) 171–180

ENGINEERING GEOLOGY

A note on thermomechanical anisotropy of clays

T. Hueckel [a] *, R. Pellegrini [b]

[a] *Duke University, Durham NC, USA*
[b] *ISMES, Bergamo, Italy*

Received 15 February 1994; accepted 23 June 1995

Abstract

Deep clays exhibit a pronounced strain anisotropy both during mechanical loading as well as during heating and cooling at constant stress in drained isotropic conditions. During mechanical loading vertical strain is larger than the horizontal one. During heating the vertical strain is larger than the horizontal one within the elastic range; the opposite is observed in the elasto-plastic range. The above described response can be interpreted adopting a consistent rotational, kinematic hardening thermo-elasto-plastic constitutive law.

1. Introduction

Anisotropy of clays is commonly due to a preferential, stable position of the platy clay particles, with their larger axis set horizontally during sedimentation and compaction. Subsequent tectonic activity may tilt and/or fold the clay layers: this effect can be considered locally through a rigid body rotation over a given angle, specified on the basis of geological data.

This paper discusses a particular aspect of clay anisotropy, that of thermo-mechanical strains. Two deep clays, the Belgian Boom clay and a deep Spanish clay, have been tested (Baldi et al., 1991; Del Olmo et al., 1996) in connection with studies aimed at assessing the possible use of clays for nuclear waste disposal. A summary of relevant properties of these clays can be found in Del Olmo et al., 1996. During mechanical tests it was noticed that both materials show a pronounced anisotropy. The ratio β of axial to lateral strain (ϵ_a,ϵ_l) observed during isotropic compression tests of the Spanish clay (Fig. 1a) and of Boom clay (Fig. 1b) calculated from the volumetric strain and axial strain readings is larger than unity and varies between 6 and 2. However, the anisotropy decreases progressively as the isotropic stress grows during re-loading; this effect is widely observed in many other materials.

Differences in the character of the relationship between temperature and axial strain on one hand and between temperature and volumetric strain on the other have been found during heating at constant stress in isotropic conditions. They suggested a closer inspection of the obtained data, with regard to anisotropy of thermal strain.

In Section 2 the test results and their interpretation are discussed. Then, in in Section 3, a rotational kinematic hardening thermo-plasticity model is presented. It is an extension of a mechanical rotational kinematic hardening model presented earlier (Hueckel and Tutumluer, 1994). Its

* Corresponding author.

0013-7952/96/$15.00
SSDI 0013-7952(95)00050-X

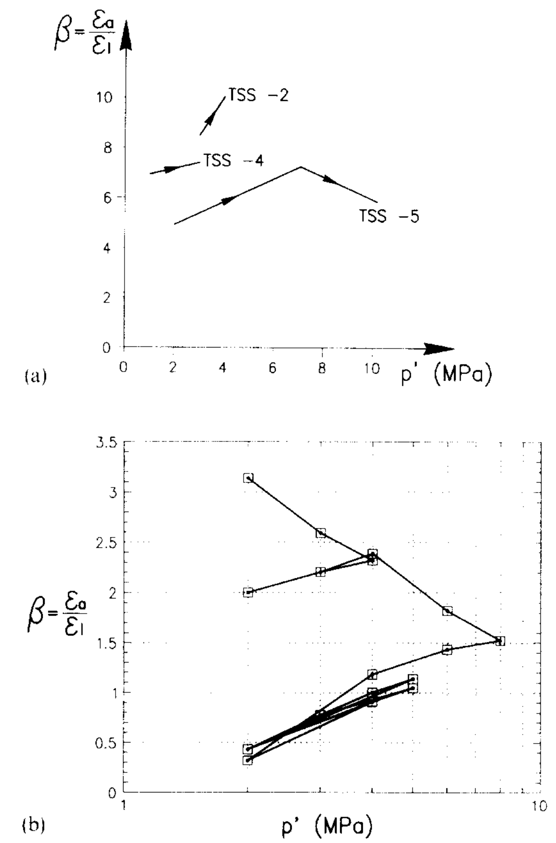

Fig. 1. (a) Ratio β of axial (ϵ_a) to lateral (ϵ_l) strain versus isotropic stress p' during isotropic compression and unloading tests TSS-2, TSS-4 and TSS-5 on a deep Spanish clay. Arrows indicate the loading path direction. (b) Ratio of axial to lateral strain β versus isotropic stress p' during the isotropic compression and unloading test TBoom-1 on deep Boom clay (Baldi et al., 1991).

athermal part includes elasto-plasticity, coupled by means of the irreversible strain accumulated during the preconsolidation process. Temperature affects the yield locus size only. A qualitative analysis of the experimental results is presented in Section 4 using the model described in Section 3.

2. Experimental results

Anisotropy of thermal strains can be best seen during isotropic heating tests. Fig. 2 shows the comparison between the measured axial strain and

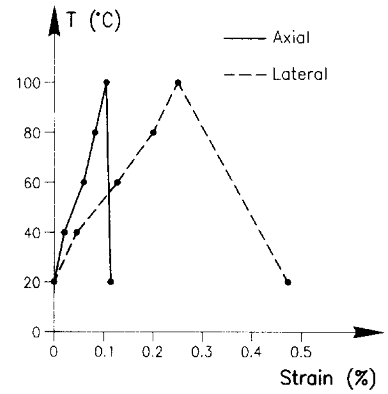

Fig. 2. Measured axial strain (solid line) and inferred lateral strain (dashed line) for test TSS-4 on a deep Spanish clay calculated as $\epsilon_l = 1/2(\epsilon_v - \epsilon_a)$; the confining effective stress is 7 MPa.

the inferred lateral strain for a deep Spanish clay (test TSS-4), while in Fig. 3 the same is presented for Boom clay (test TBoom-9). The lateral strains were obtained from the measured axial and volumetric strains. The volumetric strain is a calculated value, obtained from the volume of water expelled from the specimen and the volume of thermally expanded pore water and solid grains. A variable thermal expansion coefficient of bulk water with temperature has been used in this estimate.

As discussed elsewhere (Hueckel and Baldi, 1990), both axial and lateral strain can be dilative or contractive during heating depending on the confining pressure. This behaviour is interpreted as thermo-elastic (expansive) or thermo-plastic (contractive) according to the thermo-elastic-plastic model by Hueckel and Borsetto, 1990. Both strain components are always compressive during cooling, which in turn is interpreted as thermo-elastic.

It was also seen that for both clays, the lateral strain was larger than the axial one in all cases involving irreversible contractive strain. In test TSS-4 this occurred for heating and for cooling applied at a high confining pressure (7 MPa) with respect to the estimated maximum preconsolidation one (15 MPa). In test TBoom-9 (Fig. 3) lateral strains were larger than the axial ones at 3 MPa and at 6 MPa during heating. At 1 MPa, the vertical strain, this time expansive, was larger than that, expansive too, observed in the horizontal

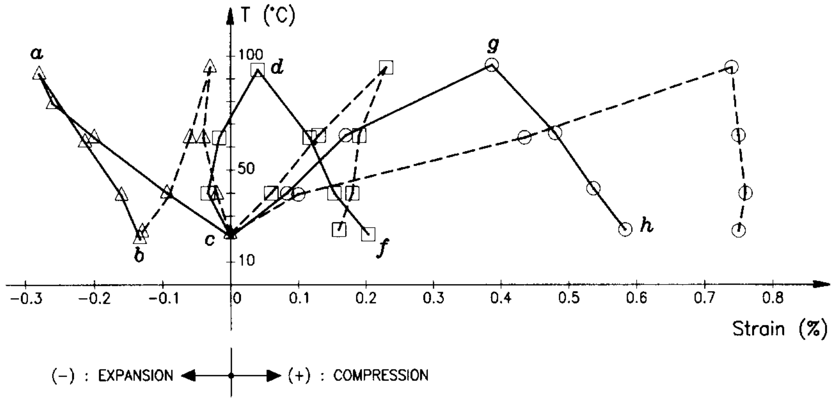

Fig. 3. Drained heating test TBoom-9 on Boom clay: axial strain versus temperature at three different confining pressures (solid line: △ = 1MPa; □ = 3MPa; ○ = 6MPa); inferred lateral strain versus temperature at three different confining pressures calculated as $\epsilon_l = 1/2(\epsilon_v - \epsilon_a)$ (dashed line: △ = 1MPa; □ = 3MPa; ○ = 6MPa) (Baldi et al., 1991).

direction. Moreover, a marked irreversible dilative vertical strain was left upon cooling the specimen back to the reference temperature at 1 MPa. The strains measured during the cooling phases of test TBoom-9 have a larger axial component. In conclusion, the thermo-plastic consolidation effect was found larger in the horizontal direction, while the reversible expansion was found larger in the vertical direction.

To avoid having the conclusions depend on the hypothesis mentioned earlier about the thermal expansion of clay water, both axial and lateral strain should be directly measured during heating. Alternatively, the lateral strain may be indirectly obtained assuming that the axial strain measured on an isotropically loaded, horizontally trimmed specimen, is identical to the horizontal strain of a vertically trimmed specimen.

For the case of Boom clay it was possible to run an additional isotropic heating/cooling test on a horizontally trimmed specimen (test TBoom-13). The specimen selected had a void ratio very close to that of TBoom-9 (0.496 vs 0.506) and the same plasticity and liquidity limits. Strains were compared at the confining pressure of 3 MPa. Again in this test, the thermo-plastic consolidation during heating was characterised by a larger horizontal component (Fig. 3, curve ***cdf***, and Fig. 4), while the thermo-elastic straining observed during cooling was characterised by a larger vertical component.

The volumetric strain has been thus calculated from the vertical strain measured during heating in tests TBoom-9 and the horizontal has been inferred from vertical strain readings in test TBoom-13. Comparing the obtained value of volumetric strain with that derived at 3 MPa from the volume of water expelled from the specimen in test TBoom-9 (Fig. 5), it was found that the volumetric strain based on these independent measures is significantly larger. The difference has been attributed to the higher thermal expansion coefficient of bulk water, used in the calculation of the volumetric strain, compared to the actual, lower, thermal expansion of pore water, see Baldi et al. (1988). Baldi et al. (1991) suggest a procedure for calibrating this effect in the evaluation of thermal strain: the volumetric strains computed according to this procedure are presented in Fig. 6a. The comparison between the lateral strain and the axial one (Fig. 6b) indicates a pronounced anisotropy of thermal strain.

Obviously, the best solution would be that of measuring the lateral strain during heating directly on the specimen using a multi-point device which could reliably operate in a high temperature environment. To the authors' knowledge, efforts to construct such device till now have not been entirely successful.

Two questions arise in relation to the experimental results presented. The first concerns the explanation of the physics of the differences observed

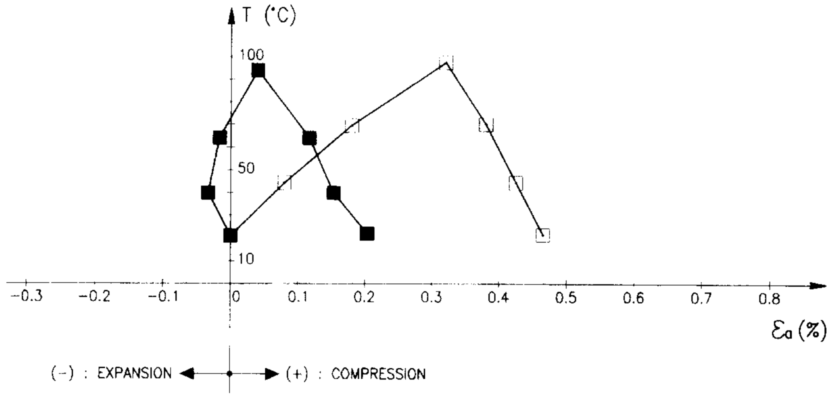

Fig. 4. Axial strain determined in the drained heating test TBoom-13 on Boom clay at 3MPa confining stress (□). This specimen has been trimmed horizontally and has similar properties to TBoom-9 specimen. Axial strain of TBoom-9 under the same test conditions are reported (■).

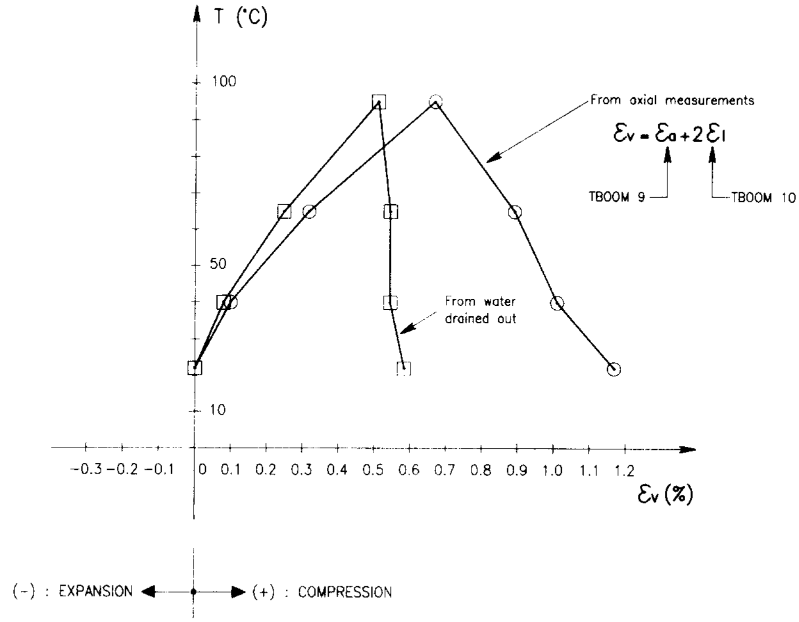

Fig. 5. Comparison between volumetric strains calculated at 3MPa from water displaced by heating and those calculated by data of Fig. 4 as $\epsilon_v = (2\epsilon_l + \epsilon_a)$.

in mechanical and thermo-mechanical anisotropy, and the second one concerns the modelling of these phenomena within a thermo-elastic-plastic model. The answer to the first query should be sought in the deformational history of the clay microstructure. The observation that during an isotropic compression, clay compacts more in the vertical than in the horizontal direction can be explained by that in its past geological loading history, the material has been subjected to a large one-dimensional, roughly vertical, compressive straining and subsequently unloaded. During these processes (Bennett and Hulbert, 1986) microstructural changes are commonly observed such as rotation and displacement of the subhorizontal packets of clay flakes, which leads to a more tightly

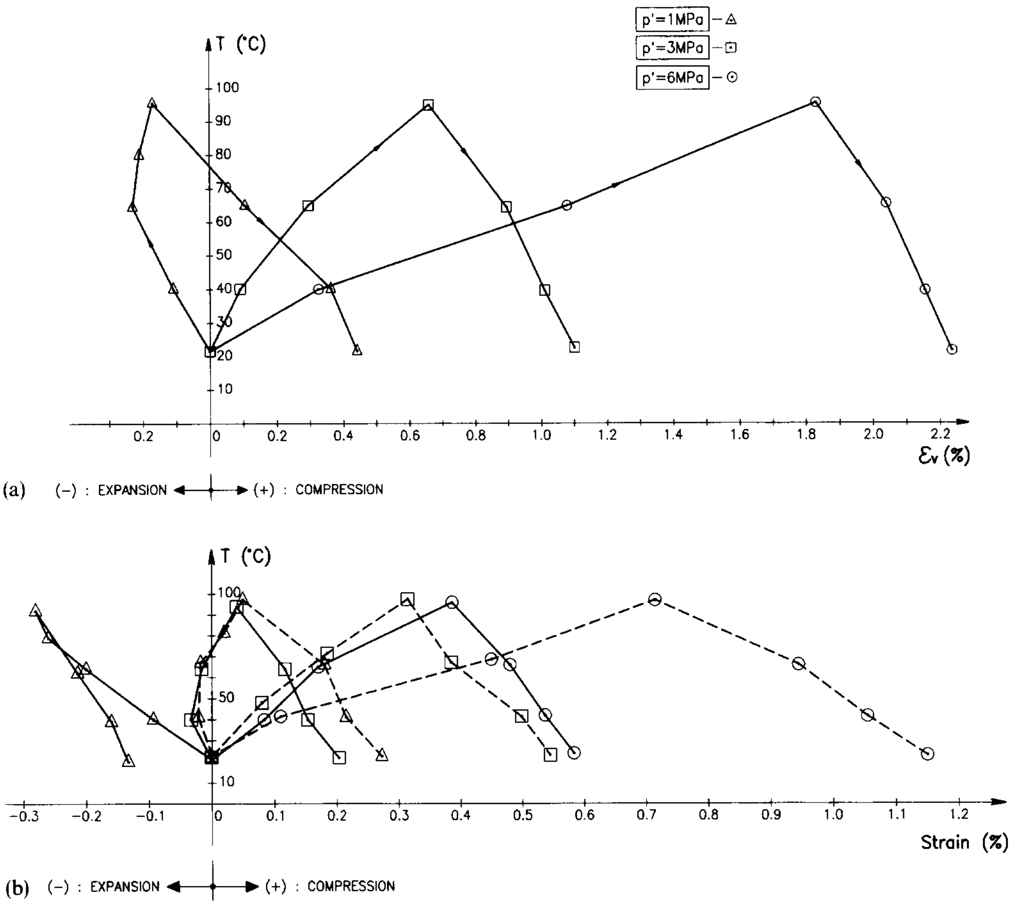

Fig. 6. (a) Volumetric strain calculated for test TBoom-9 in Boom clay (Baldi et al., 1991) accounting for the actual thermal expansion of pore water. (b) Lateral strain calculated for test TBoom-9 obtained by volumetric strain data of (a) (dashed line) as $\epsilon_l = 1/2(\epsilon_v - \epsilon_a)$, compared to the measured axial (solid line) (Baldi et al., 1991).

packed horizontal configuration during loading and a more relaxed one during unloading. As a consequence, when reloading the clay specimens as it occurs during laboratory testing, it is easier to deform them along a preferential direction (the vertical one).

The largest anisotropy is observed during elastic deformation (Mitchell, 1972), and it tends to disappear during an isotropic plastic reconsolidation. Under this condition, as observed by Griffith and Joshi (1989) most of the water contained in the macropores between clay packets is expelled, while the micropores filled with adsorbed water do not deform under mechanical load.

During heating, under isotropic conditions, the irreversible strain is larger in the horizontal direction than in the vertical one (Fig. 6b). Such an inversion of the straining mode with respect to that occurring during the geological formation process cannot be readily explained. It should be realised that the horizontal component of stress during tests run under isotropic conditions is larger than during the one-dimensional strain compaction in K_o conditions (Powers, 1967; Burst, 1969). Thus, it may be speculated that the space available in the clay microstructure after K_o compression may be mainly left between horizontally neighbouring clusters. Thus, their closure during heating at constant isotropic stress yields to larger lateral than vertical thermal straining.

3. Kinematic hardening thermo-elasto-plasticity

To model this thermal response of anisotropic clays, it is proposed to combine the thermo-elasto-plastic model described by Hueckel and Borsetto (1990) with a rotational kinematic hardening model (Baldi et al., 1991; Hueckel and Tutumluer, 1994). The latter model is devised to address the properties of anisotropy of one-dimensionally compacted and consolidated clays. For this purpose the initial yield surface is assumed to be tilted in a way that its larger semi-axis coincides with the in-situ K_o line, as suggested by Leroueil et al. (1979) and Graham et al. (1983). In the axisymmetric case, the shape of the yield surface is assumed as elliptical, Fig. 7, and its analytical expression is:

$$f=\left[\frac{p'+q\tan\theta}{a/\cos\theta}-1\right]^2+\left[\frac{q-p'\tan\theta}{Na/\cos\theta}\right]^2-1=0 \qquad (1)$$

where $p'=1/3\ (\sigma'_1+\sigma'_2+\sigma'_3)$, is the mean effective normal stress, and $q=\sqrt{3/2}\ \sqrt{S_{ij}S_{ij}}$ is the square root of the second invariant of the stress deviator $S_{ij}=\sigma_{ij}-1/3p'\delta_{ij}$ (δ_{ij} is the Kronecker delta). In the case of axisymmetric loading q is equal to the principal effective stress difference $\sigma'_1-\sigma'_3$. N is the ratio between the axes of the ellipse and θ is the angle between the ellipse's major axis and that of isotropic stress. During an active plastic or thermo-elastic-plastic process, the yield surface may undergo a further rotation governed by the kinematic hardening parameter, which depends on the deviatoric and volumetric plastic strain, but not on temperature. The representation for a general three-dimensional situation is given by Hueckel and Tutumluer (1994). The shrinking or the expansion of the yield surface depends on the volumetric plastic strain and temperature (Hueckel and Borsetto, 1990) through the strain hardening parameter, a, defined as follows:

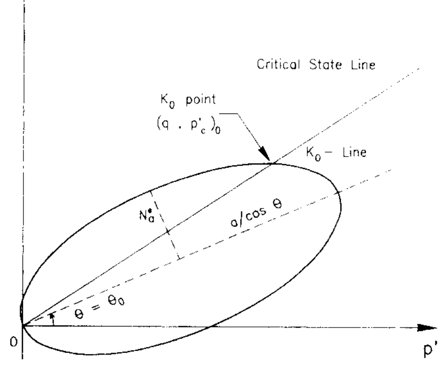

Fig. 7. Yield surface of a rotational kinematic strain hardening thermo-plastic model.

$$a=a_o\exp\left[\frac{(1+e_o)\epsilon^p_v}{\lambda-k}\right]+a_1\Delta T+a_2\Delta T^2 \qquad (2)$$

whereas the rate of rotation of the yield surface axis is defined by:

$$d(\tan\theta)=\frac{q}{p'}[\delta\exp(-\delta\epsilon^p_q)]d\epsilon^p_q+D(d\epsilon^p_v) \qquad (3)$$

where ϵ^p_v is the volumetric plastic strain and ϵ^p_q is the square root of the second invariant of plastic deviatoric strain

$$\epsilon^p_q=\sqrt{e^p_{ij}e^p_{ij}};e^p_{ij}=\epsilon^p_{ij}-1/3\epsilon^p_v\delta_{ij}$$

e_o is the initial void ratio, λ and κ are the elasto-plastic and elastic bulk logarithmic moduli, respectively, δ is a plastic anisotropy constant, a_1 and a_2 are thermal softening coefficients, D is a plastic anisotropy demise function (see Hueckel and Tutumluer, 1994).

A distinct property of clay anisotropic behavior is the strong influence of the direction of plastic strain and of its pre-strain component developed during the consolidation process which is observed in the elastic domain (elastic anisotropy, Mitchell, 1972). This can be modelled using the concept of elasto-plastic coupling (Hueckel, 1975; Maier and Hueckel, 1977, 1979). Developing this idea Hueckel and Tutumluer (1994) have assumed that the elastic moduli depend on permanent changes in the clay structure represented by the accumulated total plastic pre-strain tensor μ_{ij}. It is proposed to extend such an elasticity law, previously calibrated for kaolin and tested by Mitchell (1972), to describe thermo-elastic behaviour in the following way

$$\epsilon^{e}_{ij}=1/3\frac{\kappa}{1+e_o}\ln\left(\frac{p'}{p_o}\right)\delta_{ij}+\frac{1}{2G}(S_{ij}-S^{o}_{ij})$$
$$+C_p\ln\left(\frac{M_1}{M^{o}_1}\right)\mu_{ij}-\Delta T(\alpha^{i}\delta_{ij}+\alpha^{a}\mu_{ij}) \quad (4)$$

where M_1 and M^{o}_1 are the current and the reference value at the in-situ state of the mixed stress-plastic pre-strain invariant, respectively:

$$M_1=\sigma_{ij}\mu_{ij} \quad (5)$$
$$M^{o}_1=\sigma^{o}_{ij}\mu^{o}_{ij}$$

while the total plastic pre-strain

$$\mu_{ij}=\mu^{o}_{ij}+\int_{t_o}^{t}\frac{\partial\epsilon^{P}_{ij}}{\partial t}dt;\mu^{o}_{ij}=\int_{-\infty}^{t_o}\frac{\partial\epsilon^{P}_{ij}}{\partial t}dt \quad (6)$$

is composed of the actual plastic strain calculated from the in-situ state identified by 'time' t_o and the geological part of the pre-strain, corresponding to the entire time loading history of the soil till the onset of mechanical loading at t_o. C_p is an anisotropy constant, α^{i} and α^{a} are respectively isotropic and anisotropic temperature-dependent thermal expansion coefficients.

As a result, the elastic and thermo-elastic principal axes of strains are not coincident with those of stress, and their relative rotation is affected by the plastic pre-strain which reproduces the development of a preferential orientation of the microstructure. This effect is the anisotropy of reversible strain.

The total irreversible strain rate comprises a plastic part and a coupling part corresponding to the rate of irreversible change in elastic properties. Even if the plastic strain rate is associated, and therefore its vector is normal to the yield surface, the total irreversible strain rate becomes irreversibly deviated from the normality conditions by a vector proportional to the current plastic pre-strain vector, as follows

$$\dot{\epsilon}^{irr}_{ij}=\dot{\Lambda}\left[(1+C_pM_1)\frac{\partial f}{\partial\sigma_{ij}}+C_p\sigma_{kl}\frac{\partial f}{\partial\sigma_{kl}}\mu_{ij}\right] \quad (7)$$

where $=\dot{\Lambda}$ is the plastic multiplier. The deviation described by the last term in Eq. 7 corresponds to the anisotropy of irreversible strains.

4. Discussion

According to the above model, a uniaxially preconsolidated clay at the virgin in-situ state is characterised by a yield locus with its tip located at the maximum pre-stress point, at K_o state. When the clay is loaded isotropically, its tilted yield surface is met at a lower isotropic stress than could be predicted on the basis of a pure isotropic hardening, as implied by the original Cam-clay theory. The resulting strain rates both in the elastic and plastic domains are strongly affected by the previous one-dimensional axial precompression, as sketched in Fig. 8. It should be realised that while in general the directions of principal stresses and of principal strains do not coincide in anisotropic solids, in the triaxial apparatus their coincidence is imposed making the material transversely isotropic. This allows one to keep using the common representation of superposed stress and strain rate. The initial position of the yield surface is such that during isotropic loading the deviatoric plastic strain rate controlling its further rotation (Eq. 3) is negative and will therefore cause the surface 'righting' toward the isotropic position (Fig. 8). Moreover, the current plastic pre-strain μ_{kl} evolves with isotropic stressing. The yield surface rotating, the strain rate tends to become isotropic, leading eventually to a demise of anisotropy. This effect was seen in Boom clay and in the Spanish clay.

As for the anisotropy of thermal strains, its

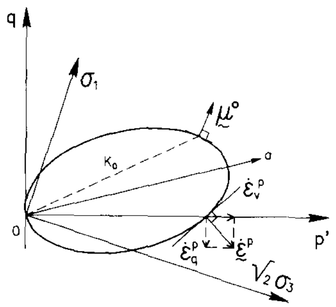

Fig. 8. Yield locus and strain rate components during isotropic loading of one-dimensionally consolidated clay.

interpretation is given using the results of the test TBoom-9 as follows. The position of the yield surface before heating at the isotropic pressure of 1 MPa corresponds to that characterising in-situ conditions (Fig. 9a). Heating induces isotropic shrinking (thermal softening) of the yield surface while initially no plastic flow and no surface rotation occur: the stress point is always still inside the elastic domain. The response is thus thermo-elastic, as described by Eq. 4, and, since $\sigma'_{ij}=\text{const.}$, it is dependent on the thermal expansion coefficients only. Its component $-\alpha^{a}\Delta T\mu_{ij}$ makes the axial tensile strain component heavily dominating in the elastic phase.

At a temperature of about 65°C the response becomes thermo-plastic. The deviatoric plastic strain is associated with the rotation of the yield surface axis from position (a) to (b) toward the isotropic axis (Eq. 3). Thermal softening is counteracted by the volumetric hardening due to

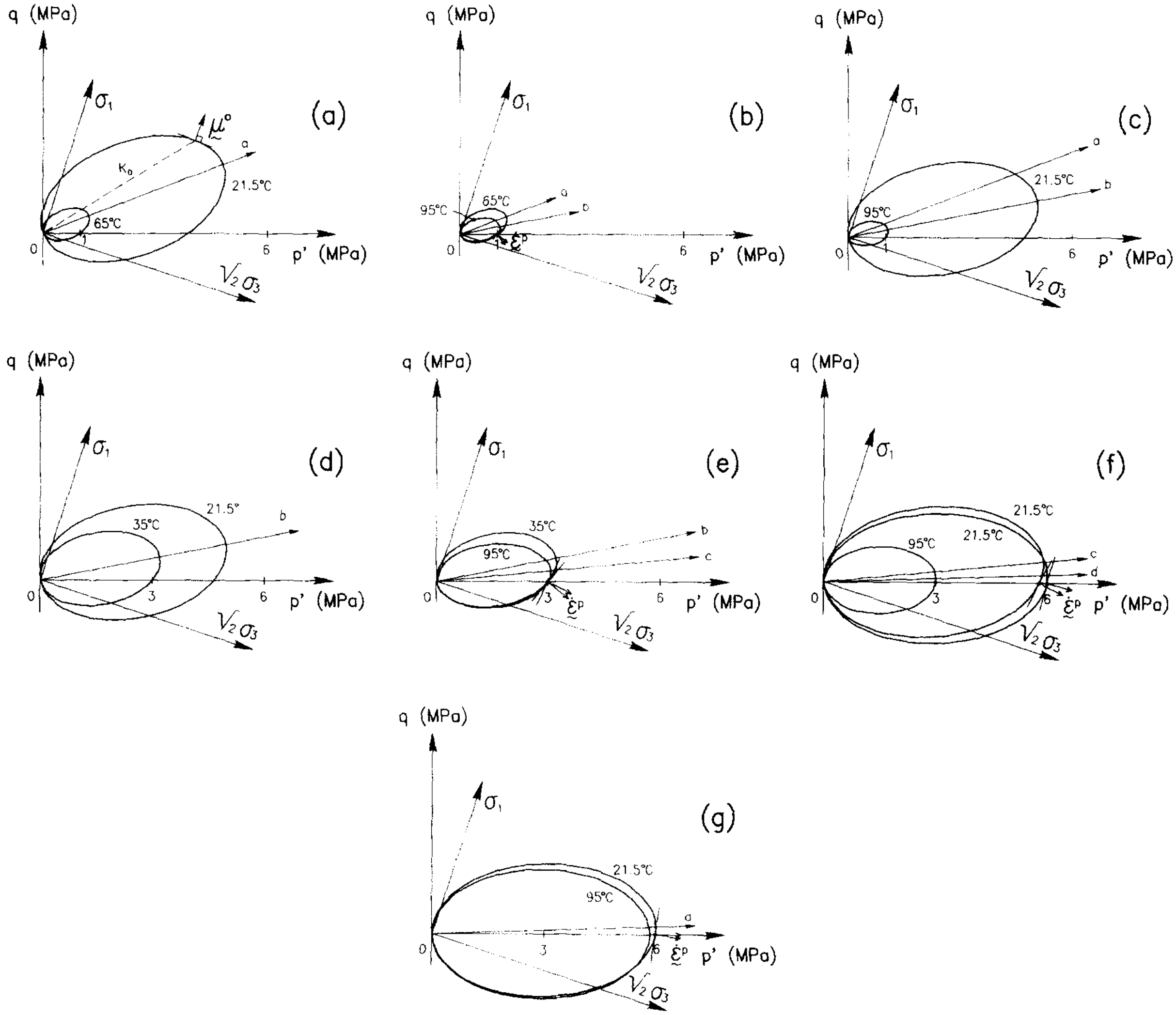

Fig. 9. History of the kinematic hardening and thermal softening of the yield surface of Boom clay to simulate its anisotropic response during test TBoom-9.

the σ'_{ij}=const. condition (Eq. 2), which results in an overall small change of yield locus' size (Fig. 9b).

The volumetric components of the irreversible strain rate are compressive, both the plastic and the coupling terms, and thus the specimen's temperature–total strain response turns towards compressive strain rates, as seen in Fig. 6a. The axial plastic strain rate value and its sign depend on the proportion in μ_{ij} between the geological pre-strain and the plastic component of the mechanical loads. The lateral strain rate is compressive all the time and numerically larger than the axial one. During cooling to 21.5°C, the yield surface expands back at constant inclination to the position sketched in Fig. 9c.

The next step in test TBoom-9 is the cooling back and the isotropic loading to 3 MPa at room temperature. It is difficult to state whether the yield surface experienced any more hardening during the isotropic loading phase. From the axial strain measured during heating at 3 MPa (Fig. 3a) it appears that until about 35°C the response is thermo-elastic, and therefore the situation is similar qualitatively to that observed during heating at 1 MPa (Fig. 9a, 9b). However, the yield surface axis (b) is now (3 MPa) less inclined (Fig. 9d) and, when yielding is reached, the corresponding plastic strain rate has a more pronounced compressive volumetric component than during heating at 1 MPa (Fig. 9e). The sign of the deviatoric plastic strain rate component implies a further rotation of the surface axis from position (b) to (c), toward the isotropic position. For both the above reasons, the global volumetric response to heating is soon plastic and compressive, and the plastic axial strain is compressive and more pronounced than it was at 1 MPa.

During cooling at 3 MPa the response is again thermo-elastic and nearly isotropic. The yield surface grows back during cooling: its axis (c) is in fact closer now to the isotropic axis than in the previous cooling at 1 MPa. Further mechanical loading to 6 MPa may imply first some elastic portion, generated by the expansion of the surface during cooling, and, subsequently, further rotational motion of the yield surface axis from position (c) to (d) during possible plastic loading. The response to thermal loading at 6 MPa may be plastic from the very beginning; indeed, as seen in Fig. 3a and Fig. 6b it is compressive in both axial and lateral directions. Numerically, the amount of plastic volumetric strain per 1°C is the largest at 6 MPa among all three heating tests. This is in agreement with the hypothesis that the yield surface is now in the least inclined position (axis d). However, a certain amount of strain rate deviation is still present.

5. Concluding remarks

The above analysis shows that a rotational kinematic hardening thermo-plastic model has a significant potential for explaining observed effects of mechanical and thermo-mechanical anisotropy. At this stage the model is understood as a guideline for setting an experimental program to study clay anisotropy. As for the experiments, a simultaneous record of axial and lateral strain is needed, and this will require reliable devices for their measurements to be developed. Calibration of the parameters of the above model requires testing of an extensive and sophisticated loading and heating history.

References

Baldi, G., Hueckel, T. and Pellegrini, R., 1988. Thermal volume changes of mineral–water system in low porosity clay soils. Can. Geotechn. J., 25(4): 807–825.

Baldi, G., Hueckel, T., Peano, A. and Pellegrini, R., 1991. Developments in modelling of thermo-hydro-geomechanical behaviour of Boom clay and clay-based buffer materials. CEC Report EUR 13365/1 and 2 EN.

Bennett, T.H. and Hulbert, M.H., 1986. Clay Microstructure. IHRDC, Boston, MA.

Burst, J.F., 1969. Diagenesis of Gulf coast clayey sediments and its possible relation to petroleum migration. Am. Assoc. Pet. Geol. Bull., 53(1): 73–93.

Del Olmo, C., Fioravante V., Gera F., Hueckel T., Mayor J.C. and Pellegrini R., 1996. Thermo-mechanical properties of deep argillaceous formations. Eng. Geol., 41 (1–4): 87–101.

Graham, J., Noonan, M.L. and Lev, K.V., 1983. Yield states and stress–strain relationships in natural plastic clay. Can. Geotech. J., 20: 502–516.

Griffith, F.J. and Joshi, R.C., 1989. Change in pore size distribution due to consolidation of clays. Geotechnique, 39(1): 159–167.

Hueckel, T., 1975. On plastic flow of granular and rock-like materials with variable elasticity. Bull. Polish Acad. Sci., Ser. Techn., 23(8): 405–414.

Hueckel, T. and Borsetto, M., 1990. Thermoplasticity of saturated soils and clays: constitutive equations. J. Geotech. Eng. Div. ASCE, 116(12): 1765–1777.

Hueckel, T. and Baldi, G., 1990. Thermoplasticity of saturated clays: experimental constitutive study. J. Geotech. Eng. Div. ASCE, 116(12): 1778–1798.

Hueckel, T. and Tutumluer, E., 1994. Modeling of elastic anisotropy due to one-dimensional plastic consolidation of clays. Comput. Geotech., 16(4): 311–349.

Leroueil, S., Tavenas, F., Brucy, F., La Rochelle, P. and Roy, M., 1979. Behaviour of destructured natural clays. J. Geotech Eng. ASCE, 105, GT6: 759–778.

Maier, G. and Hueckel, T., 1977, 1979. Non-associated and coupled flow rules of elastoplasticity for geotechnical media. Proc. 9th Int. Conf. Soil Mechanics and Foundation Eng., Tokyo, 1977; also: Int. J. Rock Mech. Min. Sci., 16: 77–92 (1979).

Mitchell, R.J., 1972. Some deviations from isotropy in a lightly overconsolidated clay. Geotechnique, 22(3): 459–467.

Powers, M.C., 1967. Fluid release mechanism in compressive marine mudrocks and their importance in oil exploration, Am. Assoc. Pet. Geol. Bull., 51(7): 1240–1254.